PHYSICAL REVIEW B VOLUME 54, NUMBER 23 15 DECEMBER 1996-I

Binding energy for the intrinsic excitons in wurtzite GaN

W. Shan, B. D. Little, A. J. Fischer, and J. J. Song
Center for Laser and Photonics Research and Department of Physics, Oklahoma State University, Stillwater, Oklahoma 74078

B. Goldenberg
Honeywell Technology Center, Plymouth, Minnesota 55441

W. G. Perry, M. D. Bremser, and R. F. Davis
Department of Materials Science and Engineering, North Carolina State University, Raleigh, North Carolina 27695

(Received 19 August 1996; revised manuscript received 27 September 1996)

We present the results of an experimental study on the binding energy for intrinsic free excitons in wurtzite GaN. High-quality single-crystal GaN films grown by metalorganic chemical vapor deposition were used in this study. Various excitonic transitions in GaN were studied using reflectance measurements. The observation of a series of spectral features associated with the transitions involving the ground and excited exciton states allows us to make a straightforward estimate of exciton binding energy using the hydrogenic model. Our results yield a binding energy $E_b=0.021\pm0.001$ eV for the *A* and *B* excitons, and 0.023 ± 0.001 eV for the *C* exciton in wurtzite GaN within the framework of the effective mass approximation. [S0163-1829(96)11948-2]

In recent years, much effort has been devoted to the study of wide-band-gap semiconductor materials and their multilayer heterostructures for optoelectronic device applications, such as laser diodes and light-emitting diodes operating in the ultraviolet-blue-green range. Currently, GaN is among the most extensively studied materials. It is known that GaN has a wurtzite structure in natural form, and has a wide direct band gap of ~3.42 eV at room temperature (300 K), which provides efficient radiative recombination and makes GaN very attractive to the short-wavelength optical applications in the blue and ultraviolet wavelength range.[1] The outstanding thermal and chemical stability of the wide-band-gap nitrides also allows GaN-based electronic and optoelectronic devices to operate at high temperatures and in hostile environments.[2,3]

So far, there have been numerous studies reporting the evidence of fine structures observed in the energy region near the band edge of GaN using various optical measurements.[4–13] In spite of these detailed studies, the description of the band structure and exciton energy levels in GaN has remained in a state of confusion. In this report we present the results of an experimental study of optical transitions associated with the ground and excited exciton states in wurtzite GaN single-crystal epilayers using conventional reflection and photomodulated reflectance (PR) measurements at low temperatures. In particular, the unambiguous observation of sharp derivativelike PR spectral features related to the 1*s* and 2*s* states of *A*-, *B*-, and *C*-exciton transitions, as well as the fundamental band-to-band (Γ_V^9-Γ_C^7) transition, allows a precise determination of the energy positions for those transitions, making it possible to directly estimate the binding energy for the excitons using the hydrogenic model. In addition, the longitudinal-transverse splitting and phenomenological damping parameter of the polaritons associated with *A* and *B* excitons were estimated by taking into account the spatial dispersion of the dielectric function of GaN.

The GaN samples used in this work were nominally undoped single-crystal films grown by metalorganic chemical vapor deposition on (0001) sapphire and 6H-SiC substrates. AlN buffer layers were deposited on the substrates at about 775 °C before the growth of the GaN epilayers. The GaN layers were deposited at 1040 °C directly on the AlN buffers. The thickness of the GaN layers ranged from 2.5 to 7.2 μm. The samples were attached to the cold finger of a closed-cycle refrigerator and cooled down to the desired temperatures for optical measurements. For conventional reflection measurements, quasimonochromatic light from a xenon lamp dispersed by a $\frac{1}{2}$-M monochromator was focused on the samples at near-normal incidence, and the reflection signals were detected using a lock-in amplification system. A chopped HeCd laser beam was used to provide optical modulation when the photomodulation measurements were performed.

Results of conventional reflection measurements taken from two samples of GaN on sapphire with epilayer thicknesses of 2.5 and 7.2 μm at 10 K are shown in Fig. 1. The reflection spectra exhibit three spectral resonances corresponding to intrinsic free-exciton transitions labeled by *A*, *B*, and *C* with the vertical arrows. The excitons referred to as the *A*, *B*, and *C* excitons are related to the Γ_9^V-Γ_7^C, Γ_7^V(upper band)-Γ_7^C and Γ_7^V(lower band)-Γ_7^C interband transitions in GaN, respectively. The *C*-exciton signature appeared weak in the spectra because the transition process, strictly speaking, is theoretically forbidden for the wave vector of the incident light along the *c* axis ($\mathbf{k}\|c$) and the polarization perpendicular to the axis ($\mathbf{E}\perp c$).[12,14] Of most interest, there is a set of weak but resolvable spectral features marked by *a* and *b* in the spectral region on the higher-energy side of the main *A* and *B* transitions in both reflection spectra. While the spectral features *A*, *B*, and *C* can be unmistakably identified to be associated with intrinsic free-exciton transitions in the spectra,[7,13] the nature of the *a* and

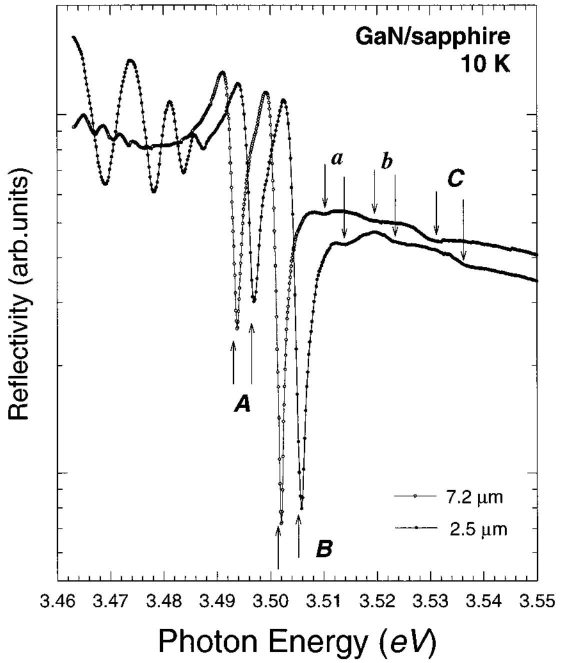

FIG. 1. Reflection spectra taken from a 2.5-μm and a 7.2-μm GaN sample at 10 K. The weak spectral structures on the reflection curves are indicated by the vertical arrows. The difference in the energy positions of A-, B-, and C-exciton resonances between two samples are caused by built-in residual strain.

b features in Fig. 1 is not immediately clear. We found that the energy separation between the a and b features is very close to the separation of the A- and B-exciton transitions. The individual distance between the A exciton and the a feature as well as the B exciton and the b feature was also found to be about the same. Similar properties were observed in the exciton spectrum of CdS by Thomas and Hopfield, which led to the determination of the binding energy for A and B excitons in the material by attributing the corresponding spectral features to $n=2$ excited exciton states based on their polarization properties.[14] However, it is very difficult to use a polarization-dependent approach in this work because of the very limited thickness of the samples used and the poor signal-to-noise ratio of the a and b features in the reflection spectra. Fortunately, photomodulation spectroscopy is an alternative approach capable of detecting weak signals so as to accurately determine their transition energies and make a positive identification for the nature of the transitions. As illustrated in Fig. 2, where photomodulated reflectance (PR) spectra taken from a sample of GaN on sapphire and a sample of GaN on SiC are given, the PR spectra not only consist of a series of sharp structures corresponding to most of the observed spectral features in the reflection spectra, but also exhibit, more strikingly, a pronounced enhancement of the barely observed weak spectral structures on the reflection curves such as the a and b features.

The difference between conventional reflection and photoreflectance is that the former is a straightforward reflectivity measurement without additional optical modulation, and the latter is a differential method utilizing modulation of the built-in electric field through photoinjected carriers by a periodically modulated light beam, such as the chopped laser beam used in this work. The change in reflectivity, $\Delta R/R$, due to the modulation may be expressed as[15]

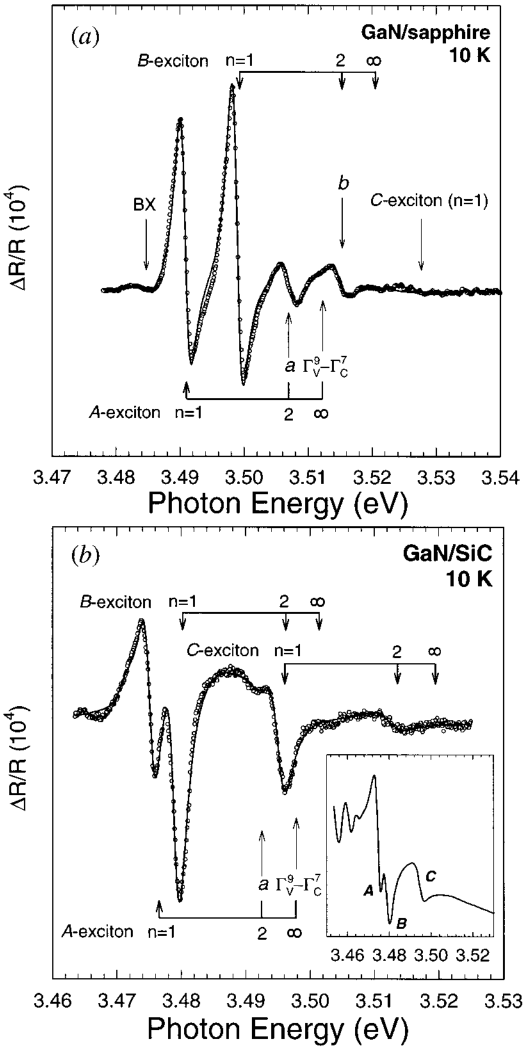

FIG. 2. 10-K PR spectrum taken from the 7.2-μm GaN/sapphire (a) and a 3.7-μm GaN/SiC (b). Open circles are experimental data, and solid lines represent the best result of the least-squares fit to the data. The identifications of the various spectral features are given by the notations.

$$\Delta R/R = a\Delta\epsilon_1 + b\Delta\epsilon_2, \tag{1}$$

where a and b are referred to as Seraphin coefficients and are related to the unperturbed dielectric function $\epsilon=\epsilon_1+i\epsilon_2$, while $\Delta\epsilon_1$ and $\Delta\epsilon_2$ are the changes in the real and the imaginary parts of the modulated dielectric function, respectively.[15] The differential changes in the reflectivity appear as sharp derivativelike line shapes in the modulated reflectance spectrum, corresponding to specific transitions in the Brillouin zone. As clearly demonstrated by Fig. 2, the weak spectral structures such as a and b could be barely observed from the conventional reflection measurement, but were greatly enhanced in the PR spectra.

In order to determine the energy positions associated with the various observed optical transitions and identify those unknown spectral features, the PR spectral features are fitted to the functional form[16–18]

$$\Delta R/R = \mathrm{Re}\left[\sum_j \{C_j e^{i\theta_j}(E-E_j+i\Gamma_j)^{-n}\}\right], \tag{2}$$

where C_j and θ_j are the amplitude and phase of the line shape, and E_j and Γ_j are the energy and the empirical broadening parameter of the transitions, respectively. The exponent n is a characteristic parameter which depends on the type of critical point and the order of the derivative. The values of $n=5/2$ and $n=2$, which correspond to three-dimensional interband and excitonic transitions, respectively,[16,19] are generally used to fit the derivativelike spectral structures. We found that the line positions and widths of the PR spectral features could only be fit using $n=2$ due to their excitonic nature. The solid lines in Fig. 2 are the best least-squares fits to the experimental data using Eq. (2). The small deviation between the fit and the experimental data on the higher-energy side of the main PR spectral features suggests that the A- and B-exciton profiles at 10 K are both inhomogeneously and homogeneously broadened. The energy positions for the A-, B-, and C-exciton transitions in the GaN/sapphire sample shown in Fig. 2(a) are 3.491, 3.499, and 3.528 eV, respectively. These values are higher than those obtained from virtually strain-free bulk GaN reported in Refs. 4–6 due to the effects of residual strain caused by the mismatch of lattice parameters and thermal expansion coefficients between the GaN epilayer and the substrate.[8,13,20] The best fits result in an energy separation of 0.008 eV between the a and b features, which is almost identical to the A-B separation, and a 0.016-eV difference for both A-a and B-b separations within experimental error ($\leqslant 0.001$ eV). Similar properties could also be observed in the other GaN samples: while the absolute energy position for the main A- and B-exciton transitions varies from sample to sample slightly due to the influence of residual strain, the energy differences of the A-a and B-b features were found to be ~ 0.016 eV for all the samples, and the energy separation between the a and b features was found to closely follow that between the main A- and B-exciton features at lower energies for each individual sample. These observations indicate that the a and b features are indeed associated with A- and B-exciton transitions. Therefore, we attribute a and b to the $n=2$ excited states $(2s)$ of the excitons. Such identifications permit a direct estimate of the binding energy for A and B excitons from the separation between the $n=1$ and $n=2$ states for excitons assuming the hydrogenic model based on the effective mass approximation is applicable. According to Elliott's theory,[21] exciton energy levels are given as

$$E_n=-E_b/n^2, \tag{3}$$

where n is an integer and E_b is the binding energy. From the results presented above, we obtain a binding energy of $E_b \approx 0.021 \pm 0.001$ eV for A and B excitons. This can be further manifested by the result of theoretical fitting to the extra spectral structure in the portion of the PR spectrum between the a and b features. We found that it is necessary to introduce one more oscillator with a third-derivative line shape to improve the fit to the experimental data. The good agreement between the theoretical fit and the observed spectrum indicates a spectral feature corresponding to a band-to-band transition at 3.512 eV. The approximate 0.021-eV energy separation from this band-to-band signature to the transition position of the $n=1$ state of the A exciton is consistent with the estimated binding energy for the exciton. Therefore, it originates from the Γ_V^9-Γ_C^7 transition, as denoted in Fig. 2(a), which corresponds to the $n=\infty$ state for the excitonic transition.

The binding energy for the C exciton can also be derived from the theoretical fitting to the PR spectrum taken from a 3.7-μm GaN sample grown on SiC as shown in Fig. 2(b) using the same approach. This sample exhibits a much stronger C-exciton transition signal in the reflection spectrum, as shown in the inset of the figure, compared to the samples of GaN on sapphire. The energy positions for the A-, B-, and C-exciton transitions in this sample are 3.470, 3.474, and 3.491 eV, respectively. In addition to the derivativelike spectral features arising from the transitions associated with the $n=1$ exciton states of the A, B, and C excitons, the spectral features related to the transitions involving the $n=2$ exciton states of the A and C excitons could be clearly observed in the PR spectrum. The best fit yields a 0.0172-eV energy separation between the $1s$ and $2s$ states of the C exciton, which corresponds to a binding energy of ~ 0.023 eV, and retains a ~ 0.016-eV difference between the A exciton $(n=1)$ and a feature as indicated in the figure.

It has to be pointed out that the exciton binding energies given above are estimated under the assumption of an isotropic reduced spherical mass for the excitons in GaN. In reality, wurtzite GaN is a hexagonal crystal with axial symmetry: the effective-mass equation for hydrogenic states should, in principle, be modified because the reduced effective mass as well as the dielectric constant is actually anisotropic. Nevertheless, the results presented here are in good agreement with the theoretical values obtained by variational calculations[22] (20.3 meV) and perturbation theory[23] (19.8 meV) based on the hydrogenic model. In addition, a reduced effective exciton mass μ can be derived from our results using the relation

$$E_b=e^4\mu/2(4\pi\hbar\epsilon)^2=13.60\mu/\epsilon^2 \ \text{eV}, \tag{4}$$

with the low-frequency dielectric constant of $\epsilon=9.5$,[24] to be $\mu \approx 0.15 m_0$. The obtained value is consistent with the value of $\sim 0.16 m_0$ estimated using an effective mass of $0.2 m_0$ for the electrons and $0.8 m_0$ for the holes in wurtzite GaN.[24] Therefore, the simple hydrogen series of Eq. (3) is still a valid approach for the determination of the binding energy for excitons in GaN.

It is known that excitons can interact strongly with photons to form a mixed state referred to as a polariton in direct-gap materials due to spatial dispersion of the dielectric constant.[25,26] It is interesting to estimate the longitudinal-transverse splitting energies and phenomenological damping parameters of the polaritons associated with A and B excitons with the consideration of spatial dispersion (i.e., the wave-vector dependence) of the dielectric function. The wave-vector-dependent dielectric function is given by[26,27]

$$\epsilon(\omega,k)=\epsilon_\infty\{1+(\omega_L^2-\omega_T^2)/(\omega_T^2-\omega^2+\beta k^2-i\omega\Gamma)\}. \tag{5}$$

Where ϵ_∞ is a frequency- and wave-vector–independent background dielectric constant, ω_T and ω_L are the transverse and longitudinal resonance frequencies at $k=0$, and Γ is the phenomenological damping constant. The spatial dispersion is described by $\beta k^2=(\hbar\omega_T/M)k^2$ with M as the effective exciton mass.[27] Figure 3 shows a comparison of the theoreti-

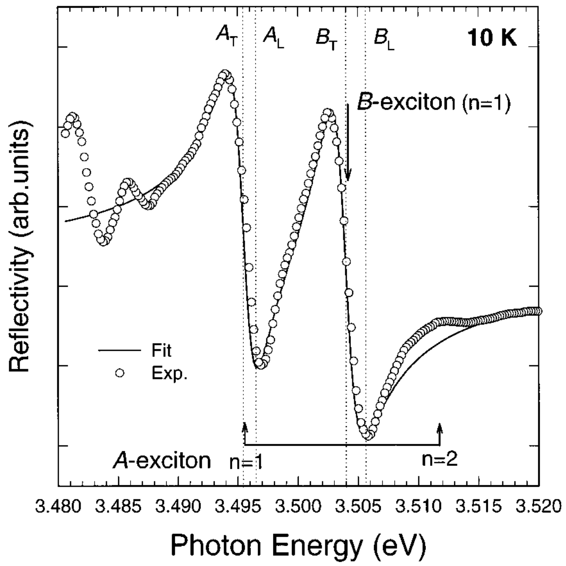

FIG. 3. Comparison of a theoretical fit taking into account spatial dispersion of the dielectric function to the 10-K reflection spectrum of 2.5-μm GaN/sapphire ($\mathbf{k} \| c$ and $\mathbf{E} \perp c$).

cal fit using Eq. (5) to the experimental spectrum taken from the 2.5-μm GaN/sapphire sample. The dotted lines in the figure indicate the energy positions of transverse and longitudinal branches of the A and B excitons. The fitting results suggest that the energy position of the transverse excitons ($\hbar\omega_T$) is an appropriate reference point for the determination of exciton binding energy within the experimental uncertainty. The best fits to the reflection spectra taken from various samples used in this work yield a longitudinal-transverse splitting $\Delta_{LT}(=\omega_L-\omega_T)\sim 0.001$ eV and a damping constant $\Gamma \sim 0.00275/\hbar$ eV for A-excitonic polaritons, and $\Delta_{LT} \sim 0.0015$ eV and $\Gamma \sim 0.003/\hbar$ eV for B-excitonic polaritons. However, these obtained values should be regarded as the lower limit for Δ_{LT} since the influence of possible mixing of A- and B-exciton states and exchange coupling due to the small energy separation was not taken into account using the simple model described by Eq. (5).

In summary, we have studied the excitonic transitions in high-quality GaN epitaxial films with the emphasis on estimating the binding energy for the intrinsic excitons in GaN. Strong, sharp derivativelike spectral structures of exciton transitions associated with the ground state and excited states of A, B, and C excitons in GaN epitaxial layers observed in photoreflectance spectra enabled us to accurately determine the transition energies and make positive identifications for those structures. Within the framework of the effective-mass approximation, we were able to make a straightforward estimate of the binding energy for these intrinsic excitons. With consideration of the spatial dispersion of the dielectric function, the longitudinal-transverse splittings and the phenomenological damping constants of A- and B-excitonic polaritons in GaN were also estimated by theoretical fitting to the conventional reflection spectra.

We are pleased to acknowledge helpful discussions with Professor X. C. Xie. This work at OSU was supported by AFOSR, DARPA, ONR, and ARO. The work at NCSU was supported by ONR under Contract No. N00014-92-J-1477.

---

[1] J. I. Pankove, in *Diamond, Silicon Carbide and Related Wide Bandgap Semiconductors*, edited by J. T. Glass, R. F. Messier, and N. Fujimori, MRS Symposia Proceedings No. 1652 (Materials Research Society, Pittsburgh, 1990), p. 515, and references therein.

[2] S. Strite and H. Morkoç, J. Vac. Sci. Technol. B **10**, 1237 (1992), and references therein.

[3] H. Morkoç, S. Strite, G. B. Gao, M. E. Lin, B. Sverdlov, and M. Burns, J. Appl. Phys. **76**, 1363 (1994).

[4] R. Dingle and M. Ilegeme, Solid State Commun. **9**, 175 (1971).

[5] R. Dingle, D. D. Sell, S. E. Stokowski, and M. Illegems, Phys. Rev. B **4**, 1211 (1971).

[6] B. Monemar, Phys. Rev. B **10**, 676 (1974).

[7] W. Shan, T. J. Schmidt, X. H. Yang, S. J. Hwang, J. J. Song, and B. Goldenberg, Appl. Phys. Lett. **66**, 985 (1995).

[8] B. Gil, O. Briot, and R.-L. Aulombard, Phys. Rev. B **52**, R17 028 (1995).

[9] M. Smith, G. D. Chen, J. Y. Lin, H. X. Jiang, M. Asif Khan, C. J. Sun, Q. Chen, and J. W. Yang, J. Appl. Phys. **76**, 7001 (1996).

[10] G. D. Chen, M. Smith, J. Y. Lin, and H. X. Jiang, S. H. Wei, M. Asif Kahn, and C. J. Sun, Appl. Phys. Lett. **68**, 2784 (1996).

[11] D. C. Reynolds, D. C. Look, W. Kim, O. Aktas, A. Botchkarev, A. Salvador, H. Morkoç, and D. N. Talwar, J. Appl. Phys. **80**, 594 (1996).

[12] S. Chichibu, A. Shikanai, T. Azuhata, T. Sota, A. Kuramata, K. Horino, and S. Nakamura, Appl. Phys. Lett. **68**, 3766 (1996).

[13] W. Shan, A. J. Fischer, J. J. Song, G. E. Bulman, H. S. Kong, M. T. Leonard, W. G. Perry, M. D. Bremser, and R. F. Davis, Appl. Phys. Lett. **69**, 740 (1996).

[14] D. G. Thomas and J. J. Hopfield, Phys. Rev. **116**, 573 (1959).

[15] D. E. Aspnes, in *Optical Properties of Solids*, edited by M. Balkanski (North-Holland, Amsterdam, 1980), Chap. 4 A.

[16] V. B. Sandomirskii, Fiz. Tverd. Tela **6**, 324 (1964) [Sov. Phys. Solid State **6**, 261 (1964)].

[17] O. J. Glembocki and B. V. Shanabrook, Superlatt. Microstruct. **3**, 235 (1987).

[18] F. H. Pollak and O. J. Glembocki, SPIE Proc. **946**, 2 (1988).

[19] H. Shen, S. C. Shen, F. H. Pollak, and R. N. Sacks, Phys. Rev. B **36**, 3487 (1987).

[20] W. Shan, R. J. Hauenstein, A. J. Fischer, J. J. Song, W. G. Perry, M. D. Bremser, R. F. Davis, and B. Goldenberg, Phys. Rev. B **54**, 13 460 (1996).

[21] R. J. Elliott, Phys. Rev. **108**, 1384 (1957).

[22] G. Mahler and U. Schröder, Phys. Status Solidi B **61**, 629 (1974).

[23] S. Xu and X. C. Xie (unpublished).

[24] *Semiconductors, Physics of Group IV Elements and III-V Compounds*, edited by K. H. Hellwage and O. Madelung, Landolt-Börnstein (Springer-Verlag, Berlin, 1982), p. 178, and references therein.

[25] S. I. Pekar, Zh. Eksp. Teor. Fiz. **33**, 1022 (1957) [Sov. Phys. JETP **6**, 785 (1958)].

[26] J. J. Hopfield and D. G. Thomas, Phys. Rev. **132**, 563 (1963).

[27] J. Lagois, Phys. Rev. B **23**, 5511 (1985).